Semiconductor Physics, Quantum Electronics & Optoelectronics, 2017. V. 20, N 3. P. 362-368.
doi: https://doi.org/10.15407/spqeo20.03.362

PACS 73.20.Mf, 87.85.fk, 81.16.Nd

Enhancing sensitivity of SPR sensors by using nanostructured Au chips coated with functional plasma polymer nanofilms

I.Z. Indutnyi[1], Yu.V. Ushenin[1], D. Hegemann[2], M. Vandenbossche[2], V.I. Myn'ko[1], P.E. Shepeliavyi[1], M.V. Lukaniuk[1], P.M. Lytvyn [1], R.V. Khrystosenko[1]
[1]V. Lashkaryov Institute of Semiconductor Physics NAS of Ukraine
41, prospect Nauky, 03680 Kyiv, Ukraine
E-mail: indutnyy@isp.kiev.ua
[2]Empa, Swiss Federal Laboratories for Materials Science and Technology,
Lerchenfeldstrasse 5, 9014 St.Gallen, Switzerland
E-mail: dirk.hegemann@empa.ch

Abstract. The sensitivity of surface plasmon resonance (SPR) sensors operating in the Kretschmann configuration was investigated using Au SPR chips with a nano-grating surface functionalized via deposition of a-C:H:O plasma polymer films. The surface of the chips was nanopatterned in order to improve the sensitivity of the sensor, as compared with the sensitivity of standard Au chips with a flat (unstructured) surface. It was found that deposition of the plasma polymer nanofilms neither affected the degree of refractometer sensitivity enhancement, nor the width of the operation range of the environment refractive index (n), in which the enhancement was observed. Such functionalization of the chip surface merely resulted in the shift of the operation range position to smaller values of n in comparison to non-coated chips requiring deposition of stable functional films.

Keywords: surface plasmon resonance, biosensor, interference lithography, plasma polymer nanolayer.

Manuscript received 22.06.17; revised version received 03.08.17; accepted for publication 06.09.17; published online 09.10.17.

1. Introduction

In recent two decades, surface plasmon resonance (SPR) sensing devices have found wide use in biosensing applications due to its advantages of high sensitivity, label-free, real-time and rapid detection. Their applications range over a large variety of fields including molecular recognition, biotechnology, medical diagnostics, drug screening *etc*. [1-6]. Most of the SPR biosensors make use of the standard Kretschmann–Raether configuration [7] to excite the surface plasmon wave in thin Au layers deposited on a transparent substrate (biosensor chip), with studied macromolecules immobilized on the Au surface. Even though SPR biosensors are more sensitive than other label-free devices, they are still unable to achieve the direct detection of small molecular species (a few hundreds of Daltons). Consequently, various proposals have been developed to enhance the sensitivity or resolution of biosensors [8, 9].

Alleyne *et al*. [10] showed theoretically that by formation of a grating at the surface of the SPR sensor chip, used in the Kretschmann–Raether configuration, the sensitivity can be improved by a factor of up to six as compared with the sensitivity of the conventional SPR sensor with a flat metallic layer. In previous works, we have experimentally demonstrated the possibility to increase the sensitivity of such SPR sensors through

formation of a periodic surface relief on the Au chip [11, 12].

Another direction for improving the performance of SPR sensors is functionalization of the Au surface for immobilization of biorecognition elements on the sensing film. The most widely used approaches include formation of self-assembled monolayers (SAMs) of alkanethiols and disulfides, or polyethylenimine (PEI) [13, 14]. However, these wet chemical treatments suffer from low layer growth rate and poor stability at enhanced temperature and UV irradiation [15].

Beside different wet-chemical methods for Au surface functionalization, plasma enhanced chemical vapor deposition offers an attractive alternative as a versatile, dry and eco-friendly technology supporting also immunosensing (detection of the reaction between an antibody and antigen) with small concentrations [16]. One of the most suitable candidates to substitute SAMs for biosensors surface modification is plasma deposition of ultrathin functional polymer films (thickness of 5…20 nm) [17, 18]. On the one hand, such thin layers should not disturb the SPR formation, and on the other hand, they should provide a substantial number of –COOH, $–NH_2$, anhydride or other reactive groups. Functional plasma polymer films, mainly comprising oxygen- or nitrogen-containing groups, are of increasing importance for biomedical applications, but also as adhesion-promoting layers [19-21]. These methods have already been successfully applied for deposition of amine-rich thin films on the surface of the gold electrode for quartz crystal microbalance biosensors [22, 23]. The response of the immunosensor functionalized via the cyclopropylamine pulsed plasma polymerization was reported to show at least 2 times better performance as compared to the standard sensor employing SAM as the intermediate layer.

In this work, both approaches were combined to investigate the sensitivity enhancement of SPR sensors operating in the Kretschmann–Raether configuration, based on Au chips with a nano-grating surface additionally coated by ultrathin a-C:H:O plasma polymer films. The optical response of the SPR refractometer depending on the grating relief and the thickness of functional plasma polymer layer were studied to show applicability of this approach using stable plasma coatings.

2. Methods

Experimental SPR chips were prepared by thermal evaporation in vacuum at the residual pressure $2\cdot10^{-3}$ Pa and subsequent deposition of an adhesive Cr layer of 3 nm in thickness, a metal (Au) layer with the thickness 40 to 50 nm, and a chalcogenide glass layer ($As_{40}S_{40}Se_{20}$) with the thickness close to 100 nm onto the substrate. For this purpose, polished 20×20×1 mm plates of glass F1 (refractive index $n = 1.615$) were used. During film deposition, the thickness was monitored using the quartz thickness meter KIT-1. After deposition, the total thickness of the film structure was measured using MII-4 microinterferometer.

For nanostructuring the gold films, we used interference (interferometric) lithography (IL) based on vacuum chalcogenide photoresist. This technology is described in more detail in previous works [11, 12]. The periodic structure (grating) was formed only on one half of the chip, whereas the other half was covered with a flat (non-structured) gold film.

A capacitively coupled, symmetric plasma reactor (Empa, Switzerland) was used for deposition of functional plasma polymer layers onto both areas (structured and flat) of the Au-coated chips. The plasma reactor configuration based on a cylindrical chamber (inner diameter of 30 cm) with plane-parallel electrodes separated by a glass ring (height of 5 cm). The upper (grounded) electrode contained the gas showerhead with several gas inlets spread over the entire electrode, while the chamber was pumped through the lower (grid) electrode coupled to the RF generator. To ensure deposition of stable plasma polymer films a gaseous mixture of CO_2 and C_2H_4 was selected at gas flow rates of 8 and 4 sccm, respectively (gas ratio 2:1), the operation gas pressure of 10 Pa, and a power input of 70 W. Functional plasma polymer nanofilms with the thickness of nominally 5 and 10 nm were deposited onto the Au SPR chips. These coatings were already characterized in a previous study [17], where a deposition rate of 6 nm·min^{-1}, a film density of 1.5 g·cm^{-3} and a [O]/[C] ratio of 21% were determined. To increase the surface reactivity, the terminal O-rich layer was deposited by increasing the CO_2/C_2H_4 ratio towards the end of the plasma process without weakening the film structure [24]. Thus, the films comprise COOH functional groups at the surface (of the order of 1 at.%).

The prepared samples were investigated using the two-channel SPR refractometer Plasmon-71 (V.Ye. Lashkaryov Institute of Semiconductor Physics NAS of Ukraine) with the operation wavelength 850 nm. The experiment was carried out in the Kretschmann–Raether configuration. For comparative studies of the sensitivity of the nanopatterned and standard sensor chips, we used solutions of glycerol (refractive index $n = 1.474$ at 20 °C) in water ($n = 1.333$ at 20 °C). The solution was introduced into the two-channel flow cuvette that was located above the two-channel chip in a way to allow the contact of the investigated liquid with the Au film. Thus, one channel of the device was responsible for the reference Au film with flat surface, while the second channel recorded the nanostructured film (with the surface relief in the form of the grating). For determination of the surface patterns of the etched periodic structure and their dimensions, a Dimension 3000 Scanning Probe Microscope (Digital Instruments Inc., Tonawanda, NY, USA) was used. The spatial frequency of the gratings was determined using the

optical stand based on the goniometer G5M with a measurement accuracy of ±5 line/mm.

3. Results and discussion

Theoretical modeling in [10] was carried out for a sinusoidal surface relief grating with a small depth of the relief. The conditions for enhancing the nanopatterned biosensor sensitivity as compared to a flat chip surface are satisfied when the period of the grating corresponds to the conditions for Bragg reflection of plasmons.

For the Au–water interface and excitation wavelength 850 nm, the Bragg resonance condition corresponds to a grating period of about 309 nm (spatial frequency, $\nu = 3240$ mm^{-1}) [12]. If the refractive index of the medium in contact with gold is larger, the resonance condition is satisfied at smaller values of the grating period. In particular, for glycerol, the Bragg resonance corresponds to a period of 277 nm ($\nu = 3610$ mm^{-1}). Based on those estimations [12], interference lithography (IL) was used to fabricate Au chips with the spatial frequency of a periodic nanorelief falling inside this range.

As an example, Fig. 1a shows the AFM image of Au grating formed by IL on the gold layer with a thickness close to 45 nm by wet etching through chalcogenide photoresist resistive mask. The period of this grating is 296.6±0.5 nm (spatial frequency $\nu = 3372$ mm^{-1}). Fig. 1b shows the same sample but coated with the nominally 10 nm thick functional plasma polymer layer. The average depth of the grating relief reached 21±2 nm after preparation (Fig. 1a) and 19±2 nm after plasma film deposition (Fig. 1b). The functional plasma polymer nanofilm, induced in this way, has only a minimal distortion of the grating relief.

The SPR refractometer Plasmon-71 allows to plot the angular dependences of the internal reflection intensity, $R(\theta)$, for a gold film to be measured and the position of the $R(\theta)$ minimum to be determined. The latter corresponds to the excitation of surface plasmons at the Au film/investigated liquid interface. The position of $R(\theta)$ minimum was found to be very sensitive to variations in n of the medium near the Au film surface, which enabled to record small changes of n. It was shown in the previous paper [12] that formation of the periodic grating on the surface of the gold chip changed the shape of reflection curve near the Bragg resonance in comparison with the same measurements using the standard Au chip. This change is consistent with the results of theoretical modeling [10]. The increase of n resulted in a shift of the position of reflectance minimum, $\Delta\theta_{min}$, toward larger angles. For nanostructured chips, this shift is higher in the same range of Δn, as compared to that of standard chips having flat surface. The sensitivity of the method is characterized by the ratio of $\Delta\theta_{min}$ to Δn. Hence, the sensitivity of the nanostructured chips is higher than that of standard chips.

The dependences of position of SPR resonance, θ_{min}, on the refractive index of the environment are shown in more detail in Figs. 2a-2c for two-channel chips, one half of which were covered with the flat, unstructured gold film and the other half obtained the surface relief in the form of Au grating with the period 302.0±0.5 nm and depth of relief 17.5±2 nm. The samples were fixed in the SPR refractometer in a way that the plane of incidence of the probing p-polarized laser beam was parallel to the grating wave vector (perpendicular to the grating grooves, *i.e.* azimuthal angle $\phi = 0$). The sample in Fig. 2a is uncoated, whereas

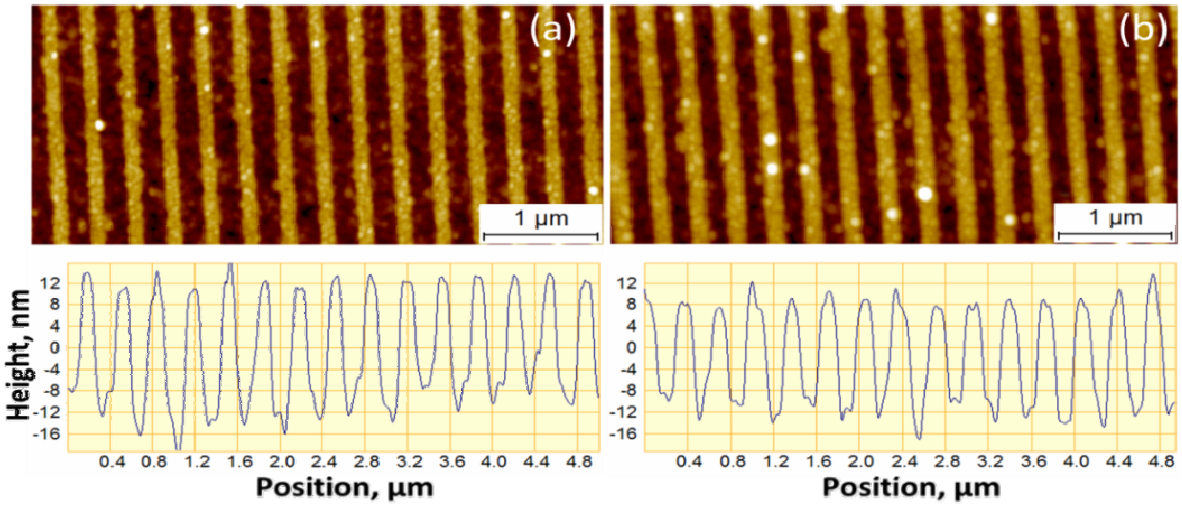

Fig. 1. AFM image and cross-sectional profile of the Au grating with the period 296.6±0.5 nm, as-prepared (*a*), and coated with a 10 nm thick functional plasma polymer layer (*b*).

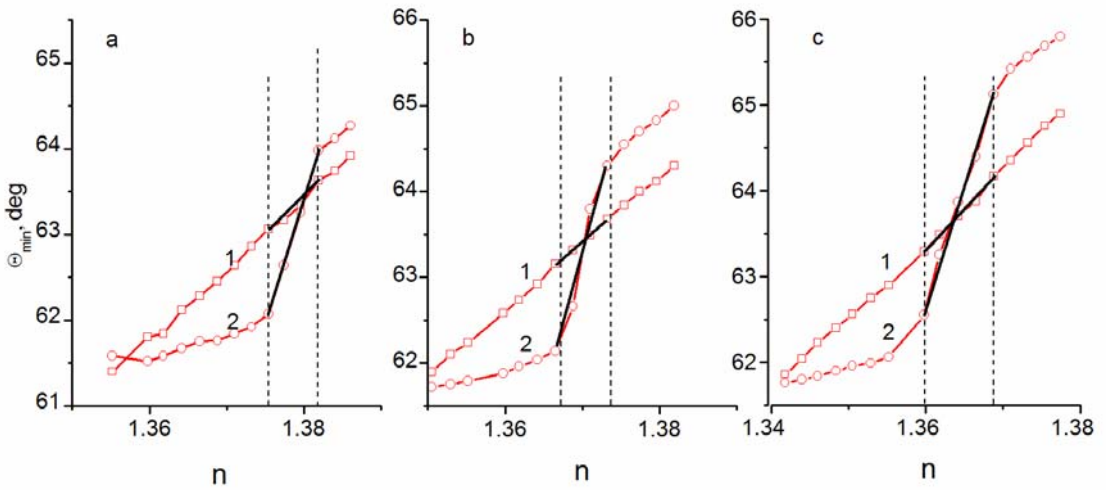

Fig. 2. The dependences of the SPR position, θ_{min}, on the refractive index of the environment, *n*, for Au standard chips with a flat surface (curve *1* in (a), (b), and (c)) and Au gratings with the period 302.0±0.5 nm and depth of relief 17.5±2 nm (curve *2* in (a), (b) and (c)). The samples in (a) are uncoated; in (b) and (c) – coated with 5 and 10 nm thick functional plasma polymer layers, respectively.

the samples in Figs. 2b and 2c are coated with 5 and 10 nm thick functional plasma polymer layers, respectively. The curves *1* in all the plots give the dependence of θ_{min} on *n* for the standard Au film with the flat (non-structured) surface. The coating thickness for the nanofilms was selected to minimize potential changes of the grating geometry before applying the uniform oxygen-functionalized surface [18].

It can be seen for the uncoated sample (Fig. 2a) that the angular position of θ_{min} on the unstructured Au film increases monotonically with the refractive index *n*, and the slope of this dependence (the ratio $\Delta\theta_{min}$ to Δn) is almost constant within the entire investigation interval of *n*. For the structured Au chip (curves *2*), the dependence of θ_{min} on *n* is nonlinear. When approaching the Bragg resonance condition, the slope of this dependence is noticeably lower in comparison with the result obtained for the standard chip. Consequently, a region with the enhanced slope (and, accordingly, with higher sensitivity) can be observed in the narrow interval of refractive index variation near Bragg resonance ($\Delta n = 0.0066$; in Fig. 2a, this section lies between two vertical dashed lines). The experimental data points obtained for both the standard and structured chips in the range of enhanced sensitivity are approximated by straight line segments. The ratio between the slopes of those segments, *i.e.*, the sensitivity ratio between the structured and standard chips, amounts to 3.6.

In our previous paper [12], it was shown that the degree of sensitivity enhancement and the range of the environment refractive index value, in which this enhancement was observed (operation range), strongly depended on the depth of the grating relief. The width of the refractive index operation range decreased with the increasing depth of relief, while the sensitivity was increased. It was found that optimum values of the relief depth for increasing the sensitivity of SPR sensors were between 10 and 23 nm. A two-to-fourfold gain in sensitivity could thus be experimentally realized for SPR biosensors by forming a grating on the operation surface of the sensor chips. Thus, for the functionalization of these grated chips, ultrathin (here: 5 and 10 nm thick) and highly stable plasma polymer films are required as described in what follows.

Figs. 2b and 2c shows how the functional plasma polymer layers deposited on the gold surfaces affects the sensitivity of the chips (both standard and nanostructured). It is seen that, for the standard Au chips by increasing the film thickness, the values of θ_{min} are increased within the entire investigation interval of *n*, as compared with the uncoated Au chip. For example, for $n = 1.36$, θ_{min} is increased from 61.46° (for uncoated Au) to 62.62° and 63.42° for coated chips with 5 and 10 nm thick plasma polymer layers, respectively. However, the slope of θ_{min} on *n* dependence, and hence the sensitivity, is not changed and remains about 100 deg/RIU (where RIU stands for refractive index unit).

Similarly, the values of θ_{min} increased with increasing the thickness of plasma polymer film on the nanostructured chips (Figs. 2b, 2c, curves *2*). In addition, the film deposition on the chip surface resulted in the shift of the operation range position by 0.0086 RIU (for 5 nm) and 0.0144 RIU (for 10 nm) to smaller values of *n* in comparison with the non-coated chips. The width of the operation range slightly increased from 0.0066 RIU for the uncoated chip to 0.0068 RIU and 0.009 RIU for the chips with 5 and 10 nm of plasma coating, respectively. The sensitivity in the operation range remained almost unchanged independently of the functionalization added to the SPR chips, giving values of 360 deg/RIU, 380 deg/RIU and 360 deg/RIU (Figs. 2a-2c, curves *2*).

Hence, the gain in sensitivity for sensor chips owing to the nanostructuring of their surface can be observed in a limited range of medium refractive index variation. This conclusion agrees with the theoretical results of ref. [10], where the enhancement was predicted in a Δn-interval narrower than 0.01. Biochemical processes investigated with SPR refractometers are often accompanied by the deposition of monolayers of biomolecules inducing very small changes in the refractive index values. Considering a refractive index resolution of SPR refractometers of $\Delta n \sim 10^{-6}$ RIU [6], the operation range Δn even less than 0.01 RIU appears to be sufficient for these measurements.

The question is how to adjust the position of the operation range with respect to the refractive index of the investigated environment. We have shown recently [12] that the most convenient method for the required adjustment might be a change in the azimuth angle. Fig. 3a shows the dependences of θ_{min} on n for the same two-channel chip as in Fig. 2b (coated with a 5 nm thick functional plasma polymer layer), but the sample was fixed in the SPR refractometer so that the plane of incidence was rotated by 4.6 degrees with respect to the grating wave vector ($\phi = 4.6°$). Fig. 3b gives the results for the same sample at $\phi = 7.5°$. It is evident that the operation range was shifted towards higher refractive indices with increasing the azimuthal angle, by 0.01 RIU at $\phi = 4.6°$ and by 0.023 RIU at $\phi = 7.5°$.

Fig. 4 displays the similar dependences for the two-channel chip coated with 10 nm thick functional plasma polymer layer (the same as in Fig. 2c). The sample was fixed in the SPR refractometer at $\phi = 6.0°$ (a) and $\phi = 11.0°$ (b). In this case, the operation range was also shifted towards higher refractive indices with increase of the azimuthal angle by 0.011 RIU at $\phi = 6.0°$ and by 0.039 RIU at $\phi = 11°$. In both cases, the increase of the azimuthal angle also induced a slightly widened operation range.

Immunosensor applications require stable surfaces, when immersion into aqueous conditions is used [15, 22, 25]. Since the applied plasma polymer thickness yields a shift of the operation range position, it is important to demonstrate that the structured chips coated with a functional plasma layer remain stable in aqueous environments, *i.e.*, unveil no film loss. Fig. 5 displays the results of the stability test in distilled water over 4 days for the sample coated with 5 nm thick a-C:H:O plasma polymer layers. Curve *1* shows the dependence of θ_{min} on n for the Au film with unstructured surface, curve *2* the same dependence for the as-prepared nanostructured chip (Au grating with the period of 302.0±0.5 nm and the depth of relief of 19±2 nm). The samples were oriented in the way that the plane of incidence was perpendicular to the grating grooves. Curve *3* finally gives the results obtained on the same sample after immersion in water. It is evident that the chip sensitivity characteristics have not changed during immersion in water (deviations between curves *2* and *3* are within measurement errors). Hence, the functional a-C:H:O films as deposited on the Au chips were found to be stable in aqueous medium for at least 4 days.

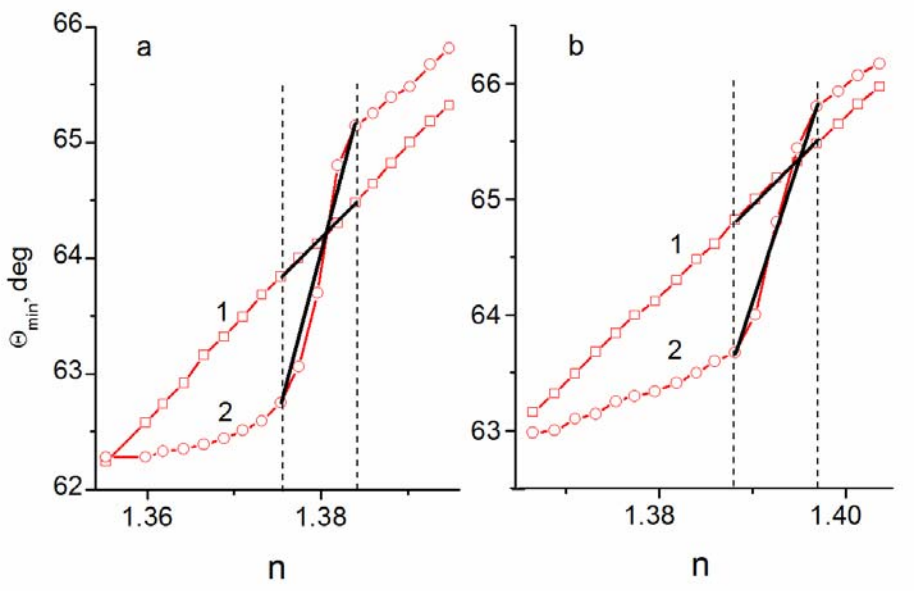

Fig. 3. The dependences of SPR position, θ_{min}, on the refractive index of the environment, n, for the Au standard sensor (curves *1*) and Au gratings with the period 302.0±0.5 nm and depth of relief 17.5±2 nm (curves *2*) coated with 5 nm thick functional plasma polymer layer: (a) $\phi = 4.6°$ and (b) $\phi = 7.5°$.

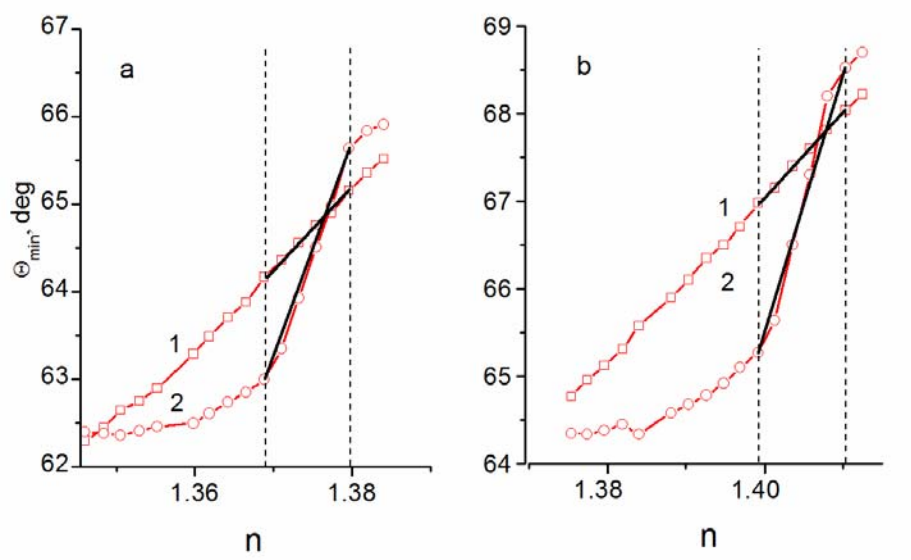

Fig. 4. The same dependences as in Fig. 3, for the identical sample coated with 10 nm thick functional plasma polymer layer: (a) $\phi = 6°$ and (b) $\phi = 11°$.

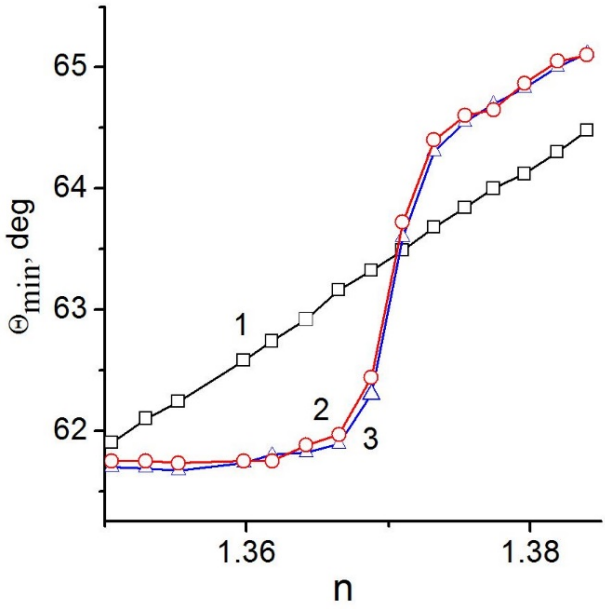

Fig. 5. The dependences of θ_{min} on n for the Au standard sensor (curves *1*) and Au grating with the period 302.0±0.5 nm and relief depth 19±2 nm, coated with 5 nm thick functional plasma polymer layer at $\phi = 0°$: as-prepared (curves *2*), and after immersion in H_2O for 96 hours (curves *3*).

4. Conclusions

The obtained results demonstrate that functionalization of the chip surface by plasma polymer nanofilms of nominal 5 and 10 nm thickness did not affect the sensitivity of SPR Au chips (both standard and nanostructured). This functionalization of the nanostructured chips with the enhanced sensitivity merely results in the shift of the operation range position to smaller values of the refractive index of the studied environment with increase in the plasma polymer film thickness. The operation range position, however, can be adjusted to the refractive index of the environment by the azimuthal rotation of the chip. Hence, with small variations of the azimuth angle, SPR measurements can be performed making use of the increased sensitivity (a two-to-fourfold gain in sensitivity can be realized) over a wide range of the refractive index changes. In addition, the plasma polymer deposition enables functionalization of the single nanostructured chip (here, with oxygen-functional groups) without deteriorating the beneficial effects due to the nanograting. These plasma polymer layers were stable in aqueous medium for at least 4 days.

Acknowledgement

The involved institutes are grateful for funding by the Swiss National Science Foundation (SNSF), grant no. IZ73Z0_152661 – SCOPES.

References

1. Maier S.A. *Plasmonics, Fundamentals and Applications*. Springer Science & Business Media, 2001, P. 224.
2. Homola J. Present and future of surface plasmon resonance biosensors. *Anal. Bioanal. Chem*. 2003. **377**. P. 528–539.
3. Gobi K.V., Tanaka H., Shoyama Y., Miura N. Continuous flow immunosensor for highly sensitive and real-time detection of sub-ppb levels of 2-hydroxybiphenyl by using surface plasmon

resonance imaging. *Biosens. Bioelectron*. 2004. **20**. P. 350–357.
4. Habauzit D., Chopineau J., Roig B. SPR-based biosensors: a tool for biodetection of hormonal compounds. *Anal. Bioanal. Chem*. 2007. **387**. P. 1215–1223.
5. Shankaran D.R., Gobi K.V.A., Miura N. Recent advancements in surface plasmon resonance immunosensors for detection of small molecules of biomedical, food and environmental interest. *Sensor. Actuat. B: Chem*. 2007. **121**. P. 158–177.
6. Ruffato G., Pasqualotto E., Sonato A., Zacco G., Silvestrie D., Morpurgo M., De Toni A., Romanato F. Implementation and testing of a compact and high-resolution sensing device based on grating-coupled surface plasmon resonance with polarization modulation. *Sensor. Actuat. B: Chem*. 2013. **185**. P. 179–187.
7. Kretschmann E. Die Bestimmung optischer Konstanten von Metallen durch Anregung von Oberflächenplasmaschwingungen. *Zeitschrift für Physik*. 1971. **24**. P. 313–324.
8. Shalabney A., Abdulhalim I. Sensitivity-enhancement methods for surface plasmon sensors. *Laser Photon. Rev.* 2011. **5**. P. 571–606.
9. Chuag S.H., Chen G.H., Chou H.H., Shen S.W., Chen C.F. Accelerated colorimetric immunosensing using surface-modified porous monoliths and gold nanoparticles. *Sci. Technol. Adv. Mater.* 2013. **14**. P. 044403.
10. Alleyne C.J., Kirk A.G., McPhedran R.C., Nicorovici N.P., Maystre D. Enhanced SPR sensitivity using periodic metallic structures. *Opt. Exp*. 2007. **15**. P. 8163–8169.
11. Dan'ko V.A., Dorozhinsky G.V., Indutnyi I.Z., Min'ko V.I., Ushenin Y.V., Korchovyi A.A., Khrystosenko R.V. Nanopatterning Au chips for SPR refractometer by using interference lithography and chalcogenide photoresist. *Semiconductor Physics, Quantum Electronics and Optoelectronics*. 2015. **18**. P. 438–442.
12. Indutnyi I., Ushenin Y., Hegemann D., Vandenbossche M., Myn'ko V., Shepeliavyi P., Lukaniuk M., Korchovyi A., Khrystosenko R. Enhancing surface plasmon resonance detection using nanostructured Au chips. *Nanoscale Res. Lett.* 2016. **11**. P. 535.
13. Fohlerova Z., Skladal P., Turanek J. Adhesion of eukaryotic cell lines on the gold surface modified with extracellular matrix proteins monitored by the piezoelectric sensor. *Biosens. Bioelectron*. 2007. **22**. P. 1896–1901.
14. Marx K. Quartz crystal microbalance: A useful tool for studying thin polymer films and complex biomolecular systems at the solution−surface interface. *Biomacromolecules*. 2003. **4**. P. 1099–1120.
15. Peluso P., Wilson D., Do D., Tran H., Venkatasubbaiah M., Quincy D., Heidecker B., Poindexter K., Tolani N., Phelan M., Witte K., Jung L.S., Wagner P., Nock S. Optimizing antibody immobilization strategies for the construction of protein microarrays. *Anal. Biochem.* 2003. **312**. P. 113–124.
16. Nakamura R., Muguruma H., Ikebukuro K., Sasaki S., Nagata R., Karube I., Pedersen H. A plasma-polymerized film for surface plasmon resonance immunosensing. *Anal. Chem.* 1997. **69**. P. 4649–4652.
17. Hegemann D., Lorusso E., Butron Garcia M.I., Blanchard N.E., Rupper P., Favia P., Heuberger M., Vandenbossche M. Suppression of hydrophobic recovery by plasma polymer films with vertical chemical gradients. *Langmuir*. 2016. **32**. P. 651–654.
18. Vandenbossche M., Butron Garcia M.I., Schütz U., Rupper P., Amberg M., Hegemann D. Initial growth of functional plasma polymer nanofilms. *Plasma Chem. Plasma Process*. 2016. **36**. P. 667–677.
19. Garcia-Fernandez M.J., Martinez-Calvo L., Ruiz J.C., Wertheimer M.R., Concheiro A., Alvarez-Lorenzo C. Loading and release of drugs from oxygen-rich plasma polymer coatings. *Plasma Process. Polym*. 2012. **9**. P. 540–549.
20. Hegemann D., Michlicek M., Blanchard N.E., Schütz U., Lohmann D., Vandenbossche M., Zajickova L., Drabik M. Deposition of functional plasma polymers influenced by reactor geometry in capacitively coupled discharges. *Plasma Process. Polym.* 2016. **13**. P. 279–286.
21. Vandenbossche M., Bernard L., Rupper P., Maniura-Weber K., Heuberger M., Faccio G., Hegemann D. Micro-patterned plasma polymer films for bio-sensing. *Mater. Design*. 2017. **114**. P. 123–128.
22. Manakhov A., Makhneva E., Skladal P., Necas D., Cechal J., Kalina L., Elias M., Zajickova L. The robust bio-immobilization based on pulsed plasma polymerization of cyclopropylamine and glutaraldehyde coupling chemistry. *Appl. Surf. Sci*. 2016. **360**. P. 28–36.
23. Makhneva E., Manakhov A., Skladal P., Zajickova L. Development of effective QCM biosensors by cyclopropylamine plasma polymerization and antibody immobilization using cross-linking reactions. *Surf. Coat. Technol*. 2016. **290**. P. 116–123.
24. Rupper P., Vandenbossche M., Bernard L., Hegemann D., Heuberger M. Composition and stability of plasma polymer films exhibiting vertical chemical gradients. *Langmuir*. 2017. **33**. P. 2340–2352.
25. Drabik M., Pesicka J., Biederman H., Hegemann D. Long-term aging of Ag/a-C:H:O nanocomposite coatings in air and in aqueous environment. *Sci. Technol. Adv. Mater*. 2015. **16**. P. 025005.